Green Reconstruction of MIL-100 (Fe) in Water for High Crystallinity and Enhanced Guest Encapsulation

Barbara E. Souza, Annika F. Möslein, Kirill Titov, James D. Taylor, Svemir Rudić, and Jin-Chong Tan*

Cite This: *ACS Sustainable Chem. Eng.* 2020, 8, 8247−8255

Read Online

| ACCESS | Metrics & More | Article Recommendations | SI Supporting Information |

ABSTRACT: MIL-100 (Fe) is a highly porous metal−organic framework (MOF), considered as a promising carrier for drug delivery and for gas separation and capture applications. However, this functional material suffers from toxic synthesis that may hinder its biomedical use and large-scale production for commercial applications. Herein, we report a "green" mechanochemical water immersion approach to yield highly crystalline MIL-100 (Fe) material. Subsequently, we have harnessed this strategy for facile fabrication of drug@MOF composite systems, comprising (guests) 5-fluorouracil, caffeine, or aspirin encapsulated in the pores of (host) MIL-100 (Fe). Inelastic neutron scattering was uniquely used to probe the guest−host interactions arising from pore confinement of the drug molecules, giving additional insights into the reconstruction mechanism. Our results pave the way for "green" production of MIL-type materials and bespoke guest-encapsulated composites by minimizing the use of toxic chemicals, while enhancing energy efficiency and the material's life cycle that is central to biotechnological applications.

KEYWORDS: Metal−organic frameworks, Mechanochemistry, Drug, Terahertz vibrations, Inelastic neutron scattering, Pore confinement
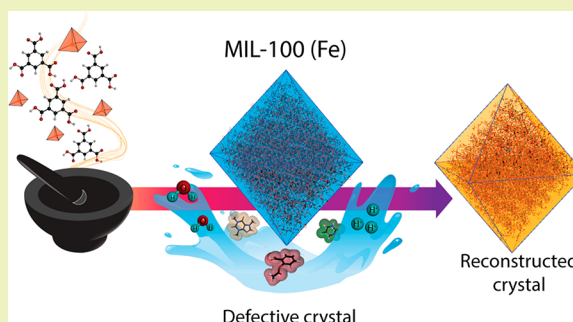
INTRODUCTION

In the vast family of metal−organic frameworks (MOFs), iron(III) carboxylate MOFs are promising given their biologically and environmentally favorable characteristics, large surface areas, and high porosity. They offer numerous coordinatively unsaturated metal sites (CUS),[1] which not only potentialize their application as drug delivery systems (DDS) but also hold great promise as adsorbents and catalysts agents.[2,3] Specifically, MIL-100 (Fe) [MIL = Materials of Institute Lavoisier] exhibits a highly ordered structure with large pores (∼3 nm), enabling the entrapment of large amounts of functional guests and drug molecules. As a functional material targeting biomedical applications, MIL-100 (Fe) features improved biocompatibility in contrast to a variety of MOFs, including its other metal counterparts, namely, MIL-100 (Cr, Ni, Cu, and Co).[4]

Thus far, there have been several different reported approaches for the fabrication of MIL-100 (Fe). Since its discovery,[5] procedures have evolved from synthesis methods with long reaction times under harsh conditions (i.e., high temperature and high pressure coupled with the use of hydrofluoric acid (HF) and concentrated nitric acid (HNO$_3$)) to high pressure solvent-free procedures.[6−9] On the one hand, the use of toxic substances, such as mineralizing agents, to improve the crystallinity of MIL-100 (Fe) material could affect its applicability in the biomedical field.[10] On the other hand, improved crystallinity is crucial as it determines the material

long-range periodicity and impacts its porosity and structural robustness. Today, one of the biggest challenges remains to optimize the synthetic procedures to yield highly crystalline MIL-100 (Fe) under mild conditions, i.e., avoiding the use of HF, toxic agents, and high pressure and temperature. The harsh methods available not only jeopardize its potential bio-oriented applications but also limit its scalability to enable commercial production. The ideal synthesis route should concomitantly allow the facile encapsulation of different (guest) drug molecules while preserving the structural properties and porosity of the (host) MIL-100 framework.

Herein, we present the use of a "green" mechanochemical approach, which is free from the need to use HF or extreme processing conditions, to yield MIL-100 (Fe) at ambient conditions. We show that the crystallinity of the material can be significantly improved upon simple immersion in water (process termed: reconstruction). Notably, the reconstruction method is highly effective for the recovery of time-degraded and mechanically amorphized samples, applicable as a material regeneration strategy. Additionally, the reconstruction step of

MIL-100 (Fe) crystals can be tailored to enable the fabrication of guest@MIL-100 composite systems (i.e., guest@MIL-100_REC). By employing a variety of drug molecules (e.g., 5-fluorouracil, caffeine, and aspirin) as guests for confinement in the pores of MIL-100 (Fe), we study the vibrational dynamics of the drug@MOF systems via inelastic neutron scattering (INS at TOSCA spectrometer).[11,12] Analysis of the collective modes unravels details behind the reconstruction process, casting new light on the guest−host interactions underpinning the controlled drug release from MOF carriers.[13]

The guest molecules were chosen based on ongoing interest in their pharmaceutical applications, yet not fully realized due to existing drawbacks. 5-Fluorouracil (5-FU) is a long-standing anticancer drug with an hydrophilic character, which restricts its passage through cell membranes without the aid of a DDS.[14] Caffeine (CAF) is widely applied as an active ingredient in many cosmetic and pharmaceutical formulations. Increasing the loading percentage of caffeine within host carriers can hugely increase its bioavailability.[15] Aspirin (ASP) is commonly used as an analgesic and anti-inflammatory drug. However, many side effects (e.g., stomach bleeding and gastrointestinal ulcers) associated with its oral administration can potentially be prevented by the use of a DDS.[16] A summary of the synthetic routes being employed in this study is illustrated in Figure 1, with full details given in the Supporting Information (SI).
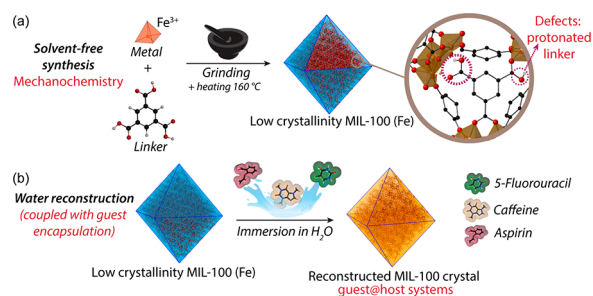

Figure 1. Schematic representation of the reconstruction method. (a) Mechanochemical approach applied to the synthesis of low crystallinity MIL-100 (Fe). (b) Reconstruction process to enhance material crystallinity and for the entrapment of different drug molecules within the MOF pores.

■ RESULTS AND DISCUSSION

Figure 2 illustrates the changes observed in MIL-100 (Fe) as a function of time throughout the reconstruction process. We have discovered that upon immersion of the low-crystallinity sample (as-synthesized) into water, it is possible to significantly enhance the material crystallinity. The sample presented a distinctive color change (Figure 2a) that was accompanied by the increase in its crystallinity, confirmed by the powder X-ray diffraction (PRXD) patterns (Figure 2b, c). The evolution in the material optical properties suggests the occurrence of microstructural changes in MIL-100 (Fe). A closer look at the diffraction data of as-synthesized MIL-100 (Fe) shows that the Bragg peaks below $2\theta = 5°$ exhibit either very low intensity or are completely absent from the pattern prior to the water reconstruction. Conversely, Bragg peaks within $2\theta = 10°−11.5°$ show a less pronounced change before and after reconstruction. The low relative intensity of the Bragg peaks at the smaller diffraction angles of $2\theta < 5°$ signifies

a weak long-range ordering of the as-synthesized MIL-100 (Fe) framework. Because the intensity of the diffraction peaks is determined by periodic atomic arrangement averaged over the entire polycrystalline sample,[17] the overall increase in intensity observed in the PXRD patterns indicates the progressive increase of long-range ordering of the MIL-100 (Fe) crystals during reconstruction.

We further assessed the structural changes by analyzing the relative peak intensity data as a function of sample immersion time (Figure 2b). The changing relative intensity of the (022):(357) planes, corresponding to the two most intense diffraction peaks, was calculated as the ratio between the peaks intensity. The results reveal a notable rise in intensity of the (022) plane (i.e., $2\theta = 4°$) versus a slower increase in intensity of the (357) plane (i.e., $2\theta = 11°$). The process can be divided into three stages. First, during the first 2 days of immersion, the relative intensity of (022):(357) peaks were marginally unaffected. In the second stage (2−7 days), we observed a steep rise in the (022):(357) relative intensity from 0.57:1 to 1:0.27, indicating a major increase in long-range periodicity of MIL-100. Finally, the relative intensity ratio stabilized, with minimal changes from 7 to 15 days. Notably, the change in the relative intensity of the peaks is accompanied by narrowing in FWHM (full width at half-maximum) of the (022) peak, indicating increasing sample crystallinity. For comparison, the normalized PXRD patterns are presented in Figure S1.

Figure 3a shows the attenuated total reflectance Fourier transform infrared (ATR-FTIR) spectra where the typical vibrational bands of MIL-100 (Fe) were detected in all samples, confirming the chemical bond integrity even in the low crystallinity material. From the ATR-FTIR spectra, two features can be highlighted. First, the sharpening of the band at ~1355 cm^{-1}, assigned to the stretching of the carboxylate groups present in the organic ligand (BTC = benzene-1,3,5-tricarboxylate), was observed (Figure S2a). This change was quantified by the decrease in FWHM of this band (Figure S2b), indicating the increase in the structural symmetry of MIL-100 (Fe) samples.[18] Second, the band at ~1720 cm^{-1}, assigned to the stretching of carboxyl group present in the acidic form of the organic linker (i.e., H_3BTC = benzene-1,3,5-tricarboxylic acid),[8,19] has shown a progressive decline in intensity, corresponding to the reduction in the spectral area of this vibrational peak (Figure S2b). These changes were accompanied by a large rise in the acidity of the solution in which MIL-100 (Fe) crystals were immersed (i.e., pH values fell from 7.4 to 2.0), as shown in Figure 2a, strongly indicating that a continuous deprotonation of the organic linker took place throughout the reconstruction process (days 1−15). A complete deprotonation of H_3BTC is required to produce a three-dimensional open framework with high crystallinity. The incomplete deprotonation of the organic ligand may obstruct the self-assembly of the secondary building units (Figure 2a), thereby resulting in partially formed (defective) mesocages. Similar results have been reported by Fernández-Bertrán et al., who obtained partially formed frameworks of $Zn(Imidazolate)_2$ via a similar manual grinding process.[20] We propose that the presence of water, acting as a weak base to form hydronium ions (H_3O^+), will facilitate the deprotonation of H_3BTC and aid in the reconstruction of the defective MIL-100 (Fe) structure resultant from the grinding process.

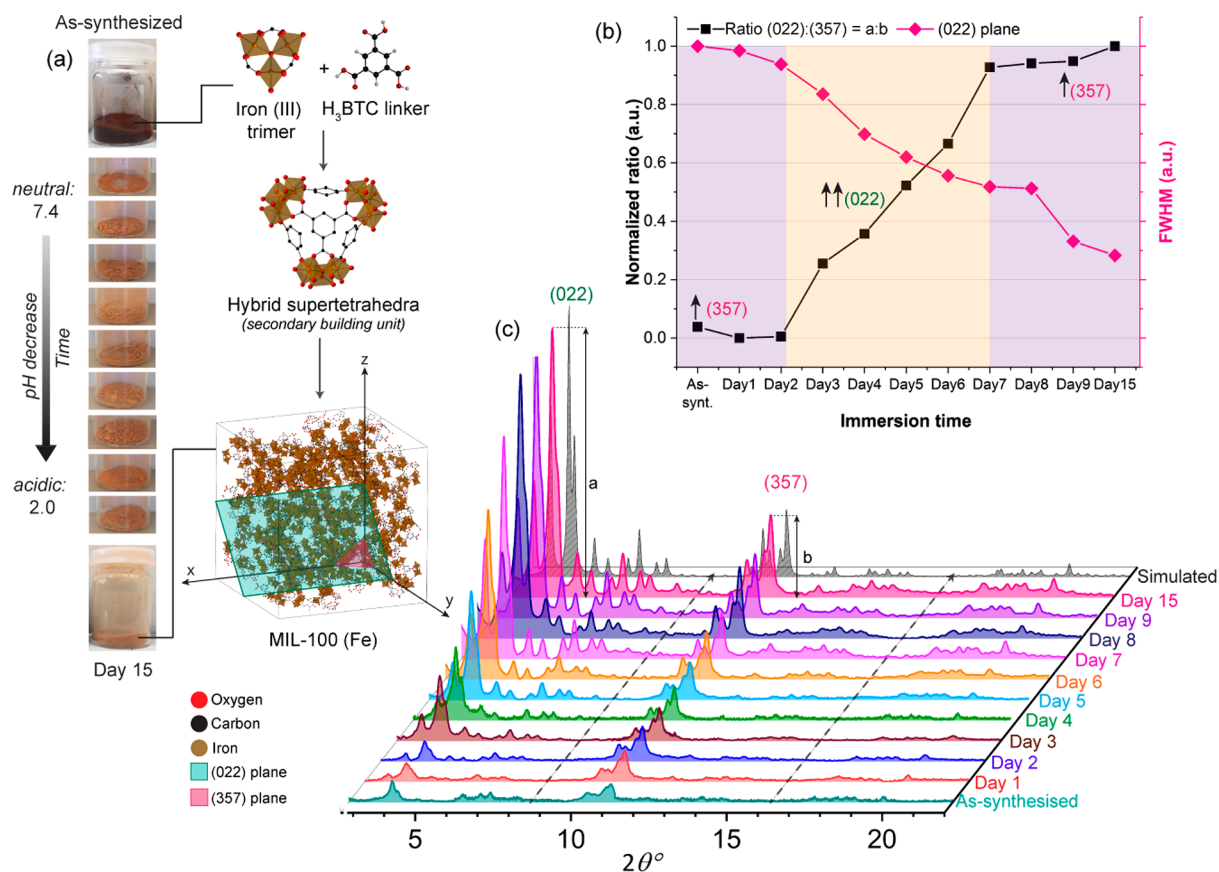To acquire a better understanding of the framework reconstruction process, we determined the Brunauer−

Figure 2. MIL-100 (Fe) reconstruction process. (a) Photographs showing evolution of the MIL-100 (Fe) samples collected at different immersion times intervals and schematics of the associated chemical structure of MIL-100 (Fe) crystals. The images display the color shift observed upon the increase of the crystallinity of MIL-100 (Fe) material. (b) Ratios of the changing relative intensity of the (022):(357) planes. The plots display a faster increase in peak intensity for small diffraction angles. The plot also presents the FWHM of the peaks corresponding to the (022) plane, showing a progressive increase in the material crystallinity. (c) Evolution of the absolute intensity of the diffraction peaks throughout the reconstruction process, showing the marked improvement in crystallinity with immersion time.

Emmett−Teller (BET) surface areas of the samples using nitrogen sorption at 77 K. The BET results of four selected samples obtained from immersion times of 2, 4, 7, and 12 days are shown in Figure 3b and Table S2. We found a considerable increase (exceeding 500%) in surface area of the Day-12 sample compared with the as-synthesized MIL-100 (Fe). Evolution of the shape of isotherms at $P/P_0 > \sim 0.7$ demonstrates the reconstruction of mesocages in MIL-100 (Fe). From the as-synthesized to Day-12 samples, one can observe the progression from type II isotherms (nonporous materials) to type I, associated with microporous materials (i.e., pore size < 2 nm), and eventually reaching type IV, attributed to mesoporous cages (i.e., pore size = 2−50 nm).[21] As shown in Figure S3 in the SI, our reconstruction method offers a good trade-off between surface area and ease of synthesis, against other reported mechanochemical, solvothermal, and solid-state strategies for synthesizing MIL-100 (Fe). For instance, the work by Pilloni et al.,[22] in which a milling approach was used in combination with corrosive tetramethylammonium hydroxide, resulted in a material with comparable surface area to our reconstructed MIL-100 (Fe). The former additive can hinder the green production of MIL-100 (Fe) in terms of energy consumption and toxicity of reactant involved in the synthesis method.

Scanning electron microscopy (SEM) and atomic force microscopy (AFM) were used to characterize the morphology

of the reconstructed samples (Figure 3c and Figures S4 and S5). We observed particles in a large range of sizes, ranging from ca. 100s of nm to 10s of μm. The grinding process appears to favor the formation of aggregates of MIL-100 (Fe) crystals, culminating in larger particles (Figure 3c) constituted from densely packed nanoparticles (Figure 3c, inset). AFM imaging (Figure 3d) revealed the granular nature of the particle surfaces, comprising nanocrystals <50 nm as depicted in Figure 3e (see Figure S5 in the SI for further details).

Exceptionally, we have demonstrated the applicability of the reconstruction process to enable the recovery of time degraded samples, which were aged for 1.5 years (Figures S6 and S7). Likewise, we discovered that mechanically amorphized samples of MIL-100 (Fe) (Figures S8 and S9) can be repaired via water reconstruction (see SI for further discussion). This is an important finding because it paves the way to the regeneration and recycling of MIL-100 materials, thereby addressing one of the main challenges preventing their industrial applications.[23,24]

Figure 4 displays the INS spectra of MIL-100 (Fe) samples collected after 2, 4, 7, and 12 days of immersion in water. Neutron scattering is a powerful spectroscopic method not subject to the optical selection rules. Unlike optical techniques such as infrared or Raman, all transitions are active in INS spectra.[25] The neutron is a highly sensitive probe to measure local changes in vibrational modes, especially low energy
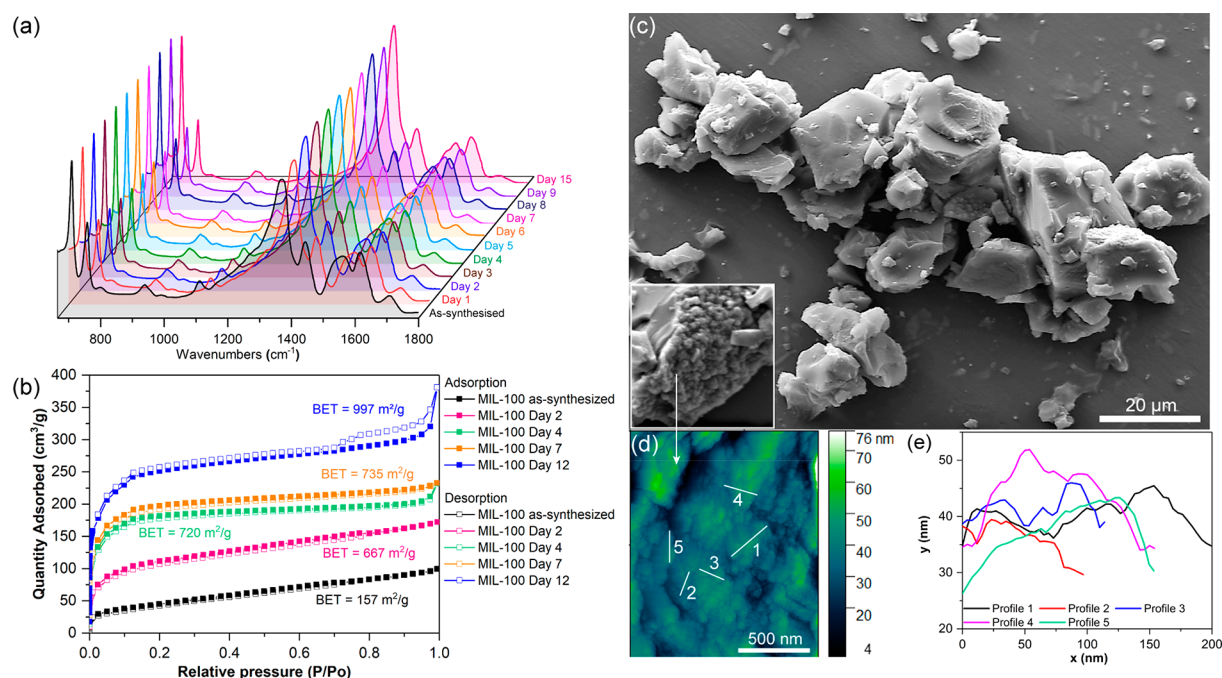
Figure 3. (a) ATR-FTIR spectra of MIL-100 (Fe) samples collected at different immersion time intervals. (b) Nitrogen adsorption and desorption isotherms of MIL-100 (Fe) samples under reconstruction. Samples were activated at 150 °C under high vacuum for 12 h prior to N_2 adsorption measurements at 77K. (c) SEM images of MIL-100 (Fe) samples. (d) AFM image displaying the surface morphology of MIL-100 (Fe) crystals accompanied by (e) the height profile of the marked regions, showing the formation of large particles by aggregation of nanosized particles.

phonons or terahertz (THz) vibrations.[26] These vibrations are collective modes associated with the lattice dynamics of the framework structure, and their analysis via INS spectroscopy can provide further insights into how the structure of MIL-100 (Fe) is rebuilt during the reconstruction process. Due to the difficulty in isolating the origin of each THz vibration in a complex system like MIL-100 (Fe), we have collected the INS spectrum of the H_3BTC linker (Figure 4a) and correlated it with density functional theory (DFT) calculations.[27] The complete comparison between experimental and theoretical spectra of H_3BTC accompanied by a description of the vibrational modes can be found in Figure S10 and Table S3. As displayed in Figure 4a, the H_3BTC molecules may establish hydrogen bonding interactions via −COOH groups. By contrasting the linker and framework spectra, we identified the modes that are predominantly influenced by the BTC linker within the framework structure of MIL-100 (Fe). A good agreement between H_3BTC and MIL-100 (Fe) spectra was observed, both in the low and high energy regions (see Figure 4b and Figure S11).

It can be seen in Figure 4b−d that the overall MIL-100 (Fe) INS spectral intensity declines with a higher sample immersion time. We can attribute this decay to two factors. First, in the INS spectrum generated on TOSCA, the intensity at low frequency (i.e., low momentum transfer (Q)) is proportional to the mean square displacement of the atoms from their equilibrium position. At higher frequency, however, the intensity is suppressed by the Debye−Waller factor.[28] On this basis, the decline in the scattering intensity in the low energy region, below 9 THz (<300 cm^{-1}), with the increase of immersion time suggests the reduction of atomic motions. As the periodicities of the MIL-100 (Fe) samples improve, we reasoned that stronger constraints are imposed onto the atomic movements in the framework. This result is substantiated by the notable rise in the thermal stability of the reconstructed

framework via thermogravimetric analysis (TGA, see Figure S12), where an ~48% increase in the initial decomposition temperature was recorded (see Table S4 for more details).

Another factor that contributes to the overall spectrum intensity is the amount of hydrogen atoms present in the sample, due to the large incoherent neutron cross-section of hydrogen atoms, the largest among all known elements.[29] We can therefore correlate the observed decrease in spectral intensity with the deprotonation of the organic linker, previously observed in the ATR-FTIR measurements (Figure S2b). As shown in the inset of Figure S11, the acidic form of the organic ligand (i.e., H_3BTC) has twice as many hydrogen atoms than its deprotonated counterpart (i.e., BTC). In the low energy region, H_3BTC vibrations are dominated by the out-of-plane bending of −COOH, including "trampoline-like" motions,[30] at 0.6−4.0 THz (20−133 cm^{-1}), out-of-plane −CO bending at ~6.4 THz (215 cm^{-1}), and ring deformation accompanied by −OH bending at ~13.8 THz (460 cm^{-1}), as illustrated in Figure 4e.[27] These vibrational modes, involving the large displacement of hydrogen atoms, show a decline in intensity upon the increase of sample immersion time, thus, the INS results support the notion that the reconstruction of MIL-100 (Fe) mesocages is controlled by the deprotonation of the organic linkers.

We have discovered that this approach can additionally be applied to fabricate highly loaded guest@host systems (termed: guest@MIL-100_REC) leading to the encapsulation of different drug molecules (guest = 5-FU, CAF, and ASP) when MIL-100 (Fe) cages are being reconstructed (experimental details are presented in the SI). SEM images of guest@MIL-100 systems reveal that the drug-loaded samples produced via the reconstruction encapsulation approach have a similar morphology to the reconstructed MIL-100 (Fe) samples (Figure S13).
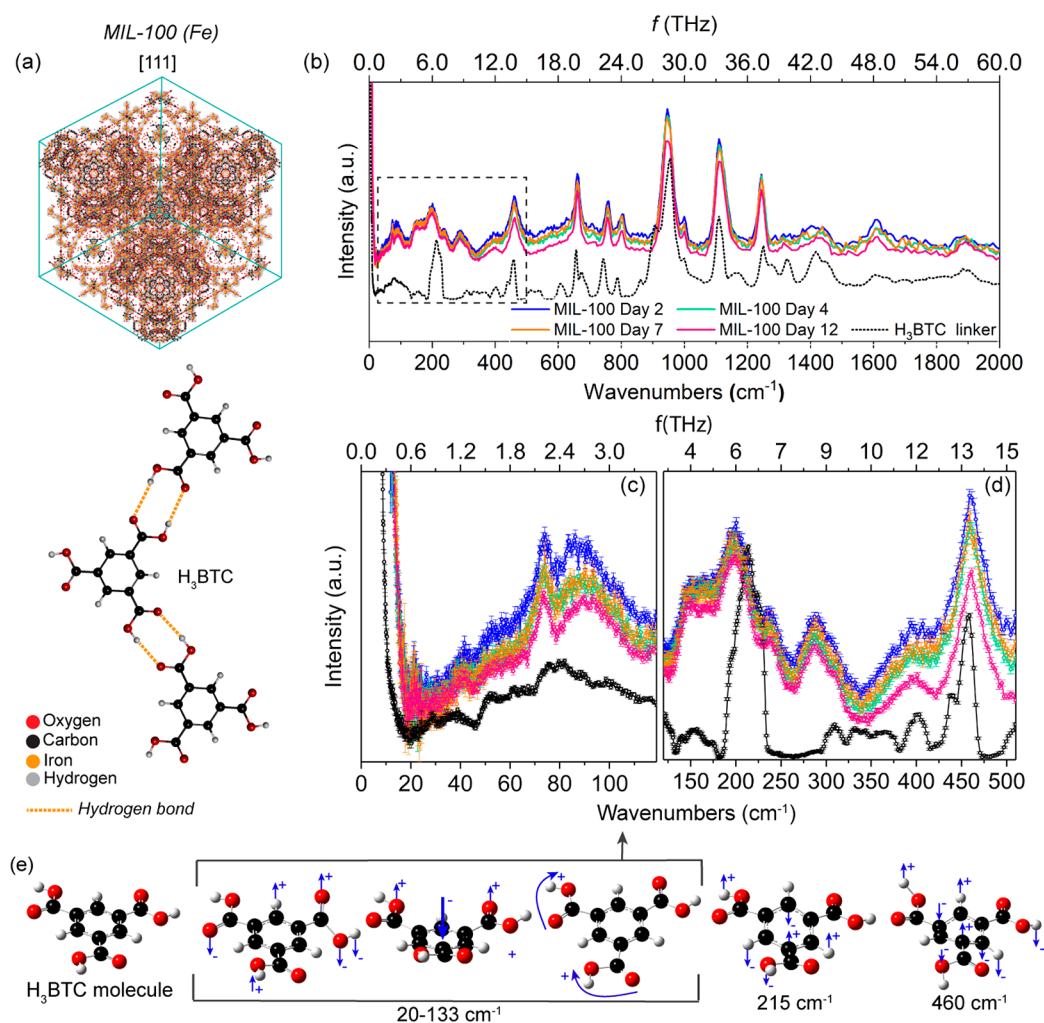
Figure 4. Inelastic neutron scattering measurements of reconstructed MIL-100 (Fe) samples. (a) Representation of MIL-100 (Fe) unit cell and H_3BTC molecules interacting via hydrogen bonds. (b) Inelastic neutron scattering (INS) spectra of MIL-100 (Fe) samples measured after different immersion times are presented against the spectrum of a H_3BTC linker (scaled down to facilitate comparison to the MIL framework spectra). Closer look at the (c) low energy region ($0-120$ cm^{-1}) and (d) $145-510$ cm^{-1} range. (e) Schematic representation of H_3BTC molecular vibrations at different wavenumbers, as simulated by DFT.

Figure 5a−c shows the PXRD patterns of drug@MIL-100 composite systems. The relative intensities of (022):(357) planes and the FWHM values of the (022) corresponding peaks of the drug@MIL-100 systems were calculated and contrasted to assess the effect that the confinement of the different drug molecules have on the crystallinity of the host material. Through the reconstruction process, 5-FU@MIL-100_REC with high crystallinity was successfully obtained. Generally, we can see that the relative peak intensity in 5-FU@MIL-100_REC (i.e., 1:0.30) agrees well with pristine MIL-100 (Fe) (1:0.24) (Figure 5a). The FWHM in Figure S14 shows that the confinement of 5-FU within MIL-100 (Fe) pores did not affect the periodicity and crystallinity of the resultant framework. A similar effect was observed in CAF@MIL-100_REC, for which the relative peak intensity (i.e., 1:0.37) and the FWHM of (022) peak were slightly larger than in 5-FU loaded counterpart but still in close agreement with the MIL-100 (Fe) pristine material (Figure 5a and Figure S14). The fabrication of ASP@MIL-100_REC was correspondingly achieved; however, the periodicity of the material was reduced when contrasted to the other drug@MIL-100 systems. After the encapsulation of aspirin, the relative intensities of the

diffraction peaks (i.e., 0.9:1) were dissimilar to the value of MIL-100 (Fe), and a large broadening of the (022) peak was detected (Figure S14). These results indicate that aspirin, in some degree, interferes with the establishment of long-range ordering of the host framework. This is because of the competition between aspirin and the H_3BTC linker molecules for coordination to the iron cations, leading to formation of an amorphous violet aspirin−iron complex known as tetraaquosalicylatroiron(III) (Figure S15).

Figure 5d−f displays the INS spectra of the drug@MIL-100 composite systems. The full spectra up to ∼60 THz (2000 cm^{-1}) are shown in Figures S16−S19. Scrutiny of the THz vibrations can provide insights on the guest−host interactions and reveal how the encapsulation of the different drug molecules affects the long-range dynamics of the host framework structure.[31] The spectra of the pure guest molecules were also collected and used for the assignment of the drug peaks in drug@MIL-100. Analysis of the INS spectra shows that in all guest−host systems considered the distinctive vibrational peaks of guest molecules were detected. This is akin to what was also observed in the high energy region, in which the ATR-FTIR spectra of the drug@MOF systems (Figure
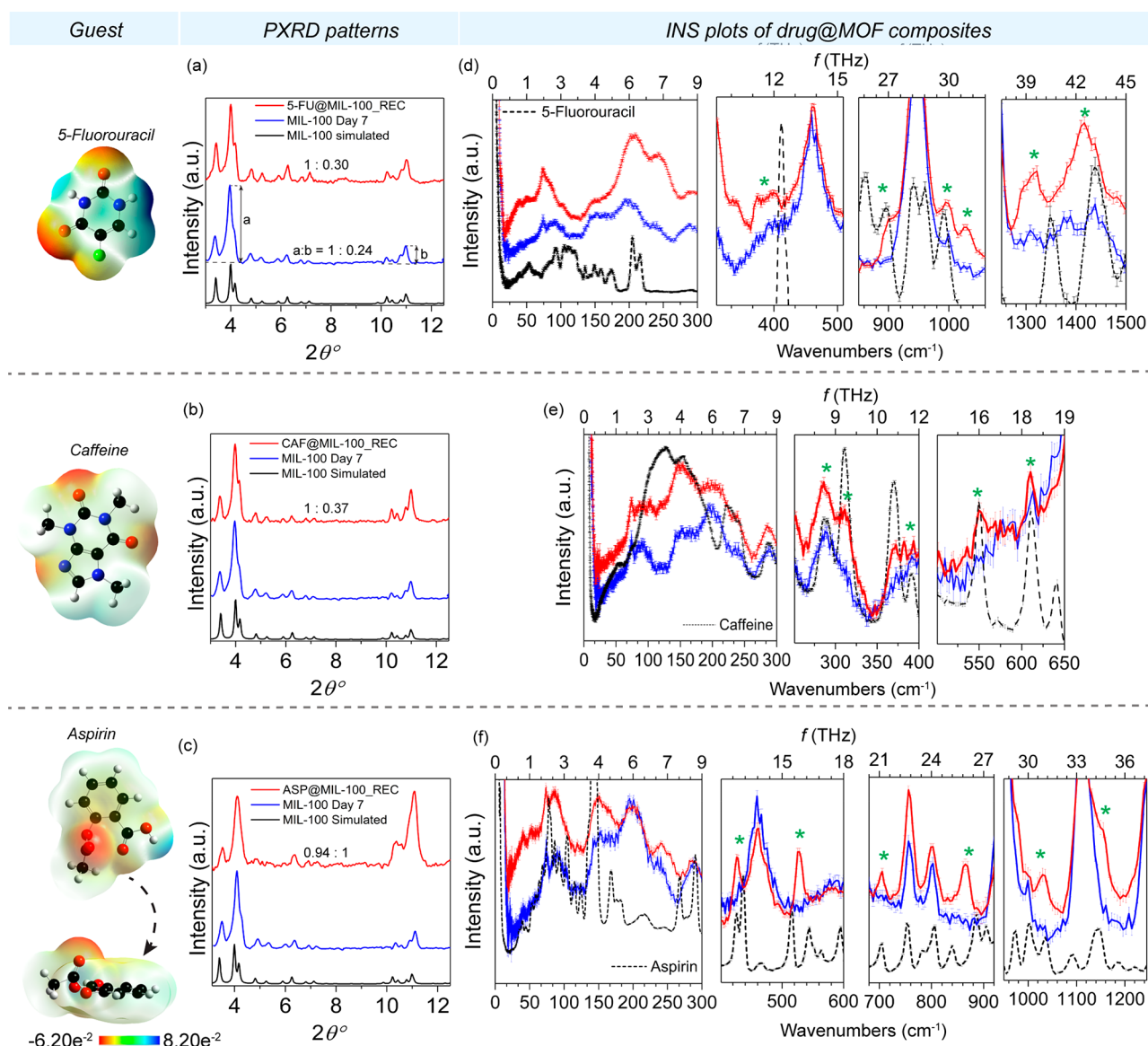
Figure 5. Powder X-ray diffraction patterns and inelastic neutron scattering (INS) spectra of drug@MIL-100 (Fe) systems. The diffraction patterns are presented for assessment of the materials crystallinity as (a) 5-FU@MIL-100_REC, (b) CAF@MIL-100_REC, and (c) ASP@MIL-100_REC. INS spectra of (d) 5-FU@MIL-100_REC, (e) CAF@MIL-100_REC, and (f) ASP@MIL-100_REC, with closer looks at the drug peaks present in the drug@MIL-100 systems, highlighted with asterisks. The guest drug molecules and their respective electrostatic potential maps (ESP) were presented, for which aspirin is shown in two different angles for better visualization. Color code: O in red, C in black, H in gray, N in navy blue, and F in green.

S20) also display the clear presence of the drug molecules. In order to correlate the influence of the guest:host ratio on the drug@MIL-100 spectra, the level of guest encapsulation was evaluated by BET surface area (Figure S21) and quantified by TGA (Figure S22). Overall, remarkably high drug loadings of 35.5 wt % (0.6 g/g MOF), 64.7 wt % (1.8 g/g MOF), and 70 wt % (2.4 g/g MOF) were achieved for 5-FU@MIL-100_REC, CAF@MIL-100_REC, and ASP@MIL-100 _REC, respectively.

The BET surface areas of the samples were found to be greatly reduced, confirming successful guest encapsulation. In Table S5, we compared the guest loading herein attained against previously reported results. In the work by Cunha et al.,[32] a theoretical approach has been used to estimate the maximum loading of caffeine molecules in MIL-100 (Fe) mesocages. A theoretical loading capacity of 65.8 wt % was

established when full accessibility of both small and large cages (i.e., 25 and 29 Å in diameter) was considered. However, using the conventional impregnation technique (i.e., immersion of the host MOF into a saturated drug solution), an experimental loading of only 49.5 wt % was attained by Cunha and co-workers. The difference between the theoretical loading capacity and the experimental loading was attributed to the nonaccessibility of caffeine molecules (7.6 × 6.1 Å) into the small cages of MIL-100 (Fe) due to the reduced size of its pentagonal window aperture (∼4.5 Å × 5.5 Å). Conversely, higher experimental loadings were achieved using our water reconstruction methodology (i.e., 64.7 wt %). As illustrated in Figure 6, instead of having to overcome the physical obstacle imposed by the narrow pore windows, the guest drug molecules get encapsulated by the formation of the MIL-100 (Fe) cages around them. This improves the occupancy of the
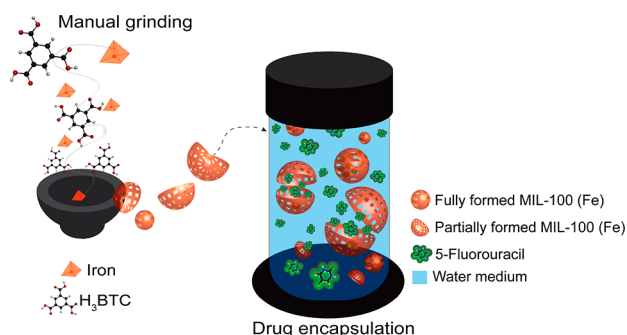
Figure 6. Schematic representation of the guest encapsulation mechanism during the reconstruction process immersed in water. The formation of the MOF cages around the drug molecules allows for the achievement of high guest loadings.

small and large cages allowing us to harness the full hosting potential of MIL-100 (Fe). The possibility of confinement of guest molecules in the small cages of MIL-100 (Fe) opens new frontiers to tuning the prolonged release of therapeutic molecules (avoiding burst effect[13] via the slow decomposition of pore cages) and to yield permanent encapsulation of bulky guests, such as fluorescent dyes for photoluminescent devices.[33]

Further insights into the dynamics of the guest−host interaction can be drawn by analyzing the INS spectra. The relatively higher intensity observed in the spectra of the guest@MIL-100_REC, specifically in the 0−9 THz (0−300 cm^{-1}) range, can be associated with a combination of scattering coming from the framework and the drug molecules. As seen in Figure 5d−f, the spectra of the drug molecules exhibit very high scattering intensities in the low energy region, meaning that even low amounts of encapsulated guest can have a large effect on the vibrational spectra of the drug@MIL-100 system.

Vibrational frequency shifts were observed in the guest vibrational modes present in the drug@MIL-100 spectra (marked in Figure 5d−f by asterisks). Such shifts indicate the existence of constraints to free motions of the drug molecule. For example, the effect of the guest confinement is evident on the 5-FU@MIL-100_REC spectrum, in which the very strong 5-FU vibration at ~12.3 THz (~410 cm^{-1}) associated with the in-plane bending of OCNCO is highly suppressed (Figure S23).[34] On the basis of the electrostatic potential surface map (ESP) depicted in Figure 5, 5-FU molecules will bind to the CUS via one of their oxygen atoms through Fe−O coordination. The same scenario is repeated for caffeine and aspirin molecules, which as shown in the ESP maps in Figure 5 can also establish Fe−O coordination to the host MIL-100 (Fe) CUS. Similarly, the suppression and shift of the caffeine modes at ~10.8 THz (~360 cm^{-1}) related to C=O bending and the shift of aspirin modes at ~12.6 THz (~421 cm^{-1}) and ~16.0 THz (~533 cm^{-1}) related to the C=O bending substantiates the formation of Fe−O coordination between caffeine and aspirin to the CUS. The shift of the aspiring modes at ~25.6 THz (~855 cm^{-1}) and ~31.2 THz (~1040 cm^{-1}), associated with benzene ring deformation, suggests that the drug molecules simultaneously form π−π interactions with the organic linker and between drug molecules within MIL-100 (Fe) cages. In fact, comparing the sizes of MIL-100 (Fe) mesocages (25 and 29 Å in diameter),[5] the chosen drug molecules are considerably small (Figure

S24), meaning that the interactions between multiple drug molecules (e.g., dimers formation) are expected inside the same pore. The suppression and shifts of high intensity drug molecule modes indicate a strong guest−host interaction yielded by the employment of the reconstruction encapsulation method.

■ CONCLUSIONS

In summary, we have demonstrated the use of a low cost, green mechanochemical method applied to the facile fabrication of highly crystalline MIL-100 (Fe) material, where framework reconstruction in water leads to improved thermal stability. This approach can be used to achieve guest@MIL-100 systems with a high loading of the encapsulated guest molecules. High-resolution inelastic neutron scattering spectroscopy aided the understanding of the guest−host interactions by unravelling the vibrational dynamics of the MIL-100 (Fe) phase and its guest-encapsulated composites. This work provides new approaches toward the eco-friendly and scalable synthesis of mesoporous MIL-100 (Fe) and guest@MIL-100 systems, avoiding the use of highly toxic agents that are limiting the promising biomedical applications of MIL-100 (Fe). The simple approach demonstrated here could be applied to the large-scale synthesis of mesoporous MIL-100 materials for future commercialization.

■ ASSOCIATED CONTENT

ⓢ Supporting Information
The Supporting Information is available free of charge at https://pubs.acs.org/doi/10.1021/acssuschemeng.0c01471.

> Synthetic procedures in detail, DFT calculations, materials characterization (TGA, SEM, AFM, and PXRD), and drug encapsulation studies. (PDF)

■ AUTHOR INFORMATION

Corresponding Author
Jin-Chong Tan − *Multifunctional Materials & Composites (MMC) Lab, Department of Engineering Science, University of Oxford, Oxford OX1 3PJ, United Kingdom;* ⓞ orcid.org/0000-0002-5770-408X; Email: jin-chong.tan@eng.ox.ac.uk

Authors
Barbara E. Souza − *Multifunctional Materials & Composites (MMC) Lab, Department of Engineering Science, University of Oxford, Oxford OX1 3PJ, United Kingdom;* ⓞ orcid.org/0000-0001-6315-2149

Annika F. Möslein − *Multifunctional Materials & Composites (MMC) Lab, Department of Engineering Science, University of Oxford, Oxford OX1 3PJ, United Kingdom*

Kirill Titov − *Multifunctional Materials & Composites (MMC) Lab, Department of Engineering Science, University of Oxford, Oxford OX1 3PJ, United Kingdom*

James D. Taylor − *STFC Rutherford Appleton Laboratory ISIS Neutron and Muon Source Chilton, Didcot OX11 0QX, United Kingdom*

Svemir Rudić − *STFC Rutherford Appleton Laboratory ISIS Neutron and Muon Source Chilton, Didcot OX11 0QX, United Kingdom*

Complete contact information is available at:
https://pubs.acs.org/10.1021/acssuschemeng.0c01471

Notes

The authors declare no competing financial interest.

■ REFERENCES

(1) García Márquez, A.; Demessence, A.; Platero-Prats, A. E.; Heurtaux, D.; Horcajada, P.; Serre, C.; Chang, J.-S.; Férey, G.; de la Peña-O'Shea, V. A.; Boissière, C.; Grosso, D.; Sanchez, C. Green Microwave Synthesis of MIL-100(Al, Cr, Fe) Nanoparticles for Thin-Film Elaboration. *Eur. J. Inorg. Chem.* 2012, 2012, 5165−5174.

(2) Tian, H.; Peng, J.; Du, Q.; Hui, X.; He, H. One-Pot Sustainable Synthesis of Magnetic Mil-100(Fe) with Novel Fe_3O_4 Morphology and Its Application in Heterogeneous Degradation. *Dalton Trans.* 2018, 47, 3417−3424.

(3) Zhang, C. F.; Qiu, L. G.; Ke, F.; Zhu, Y. J.; Yuan, Y. P.; Xu, G. S.; Jiang, X. A Novel Magnetic Recyclable Photocatalyst Based on a Core-Shell Metal-Organic Framework Fe_3O_4@MIL-100(Fe) for the Decolorization of Methylene Blue Dye. *J. Mater. Chem. A* 2013, 1, 14329−14334.

(4) Horcajada, P.; Chalati, T.; Serre, C.; Gillet, B.; Sebrie, C.; Baati, T.; Eubank, J. F.; Heurtaux, D.; Clayette, P.; Kreuz, C.; Chang, J. S.; Hwang, Y. K.; Marsaud, V.; Bories, P. N.; Cynober, L.; Gil, S.; Ferey, G.; Couvreur, P.; Gref, R. Porous Metal-Organic-Framework Nanoscale Carriers as a Potential Platform for Drug Delivery and Imaging. *Nat. Mater.* 2010, 9, 172−178.

(5) Horcajada, P.; Surble, S.; Serre, C.; Hong, D. Y.; Seo, Y. K.; Chang, J. S.; Greneche, J. M.; Margiolaki, I.; Ferey, G. Synthesis and Catalytic Properties of MIL-100(Fe), an Iron(III) Carboxylate with Large Pores. *Chem. Commun.* 2007, 2820−2822.

(6) Yuan, B.; Wang, X.; Zhou, X.; Xiao, J.; Li, Z. Novel Room-Temperature Synthesis of MIL-100(Fe) and Its Excellent Adsorption Performances for Separation of Light Hydrocarbons. *Chem. Eng. J.* 2019, 355, 679−686.

(7) Han, L.; Qi, H.; Zhang, D.; Ye, G.; Zhou, W.; Hou, C. M.; Xu, W.; Sun, Y. Y. A Facile and Green Synthesis of MIL-100(Fe) with High-Yield and Its Catalytic Performance. *New J. Chem.* 2017, 41, 13504−13509.

(8) Mahmoodi, N. M.; Abdi, J.; Oveisi, M.; Alinia Asli, M.; Vossoughi, M. Metal-Organic Framework (MIL-100 (Fe)): Synthesis, Detailed Photocatalytic Dye Degradation Ability in Colored Textile Wastewater and Recycling. *Mater. Res. Bull.* 2018, 100, 357−366.

(9) Seo, Y.-K.; Yoon, J. W.; Lee, J. S.; Lee, U. H.; Hwang, Y. K.; Jun, C.-H.; Horcajada, P.; Serre, C.; Chang, J.-S. Large Scale Fluorine-Free Synthesis of Hierarchically Porous Iron(III) Trimesate MIL-100(Fe) with a Zeolite Mtn Topology. *Microporous Mesoporous Mater.* 2012, 157, 137−145.

(10) Fang, Y.; Wen, J.; Zeng, G.; Jia, F.; Zhang, S.; Peng, Z.; Zhang, H. Effect of Mineralizing Agents on the Adsorption Performance of Metal-Organic Framework MIL-100(Fe) Towards Chromium(VI). *Chem. Eng. J.* 2018, 337, 532−540.

(11) Parker, S. F.; Fernandez-Alonso, F.; Ramirez-Cuesta, A. J.; Tomkinson, J.; Rudic, S.; Pinna, R. S.; Gorini, G.; Fernández

Castañon, J. Recent and Future Developments on TOSCA at ISIS. *J. Phys.: Conf. Ser.* 2014, 554, 012003.

(12) Pinna, R. S.; Rudić, S.; Parker, S. F.; Armstrong, J.; Zanetti, M.; Škoro, G.; Waller, S. P.; Zacek, D.; Smith, C. A.; Capstick, M. J.; McPhail, D. J.; Pooley, D. E.; Howells, G. D.; Gorini, G.; Fernandez-Alonso, F. The Neutron Guide Upgrade of the TOSCA Spectrometer. *Nucl. Instrum. Methods Phys. Res., Sect. A* 2018, 896, 68−74.

(13) Souza, B. E.; Dona, L.; Titov, K.; Bruzzese, P.; Zeng, Z.; Zhang, Y.; Babal, A. S.; Moslein, A. F.; Frogley, M. D.; Wolna, M.; Cinque, G.; Civalleri, B.; Tan, J. C. Elucidating the Drug Release from Metal-Organic Framework Nanocomposites Via in Situ Synchrotron Microspectroscopy and Theoretical Modelling. *ACS Appl. Mater. Interfaces* 2020, 12, 5147−5156.

(14) Hou, J.; Li, C.; Cheng, L.; Guo, S.; Zhang, Y.; Tang, T. Study on Hydrophilic 5-Fluorouracil Release from Hydrophobic Poly-(Epsilon-Caprolactone) Cylindrical Implants. *Drug Dev. Ind. Pharm.* 2011, 37, 1068−1075.

(15) Liédana, N.; Lozano, P.; Galve, A.; Téllez, C.; Coronas, J. The Template Role of Caffeine in Its One-Step Encapsulation in MOF NH_2-MIL-88b(Fe). *J. Mater. Chem. B* 2014, 2, 1144−1151.

(16) Singco, B.; Liu, L.-H.; Chen, Y.-T.; Shih, Y.-H.; Huang, H.-Y.; Lin, C.-H. Approaches to Drug Delivery: Confinement of Aspirin in MIL-100(Fe) and Aspirin in the De Novo Synthesis of Metal-Organic Frameworks. *Microporous Mesoporous Mater.* 2016, 223, 254−260.

(17) Sivia, D. S. *Elementary Scattering Theory: For X-Ray and Neutron Users*; Oxford University Press: Oxford, U.K., 2011.

(18) Petit, C. *Factors Affecting the Removal of Ammonia from Air on Carbonaceous Materials: Investigation of Reactive Adsorption Mechanism*; Springer Science & Business Media: New York, 2012.

(19) Lin, S.; Song, Z.; Che, G.; Ren, A.; Li, P.; Liu, C.; Zhang, J. Adsorption Behavior of Metal-Organic Frameworks for Methylene Blue from Aqueous Solution. *Microporous Mesoporous Mater.* 2014, 193, 27−34 27−34.

(20) Fernández-Bertrán, J. F.; Hernández, M. P.; Reguera, E.; Yee-Madeira, H.; Rodriguez, J.; Paneque, A.; Llopiz, J. C. Characterization of Mechanochemically Synthesized Imidazolates of Ag^{+1}, Zn^{+2}, Cd^{+2}, and Hg^{+2}: Solid State Reactivity of Nd^{10} Cations. *J. Phys. Chem. Solids* 2006, 67, 1612−1617.

(21) Thommes, M.; Kaneko, K.; Neimark, A. V.; Olivier, J. P.; Rodriguez-Reinoso, F.; Rouquerol, J.; Sing, K. S. W. Physisorption of Gases, with Special Reference to the Evaluation of Surface Area and Pore Size Distribution. *Pure Appl. Chem.* 2015, 87, 1051−1069.

(22) Pilloni, M.; Padella, F.; Ennas, G.; Lai, S.; Bellusci, M.; Rombi, E.; Sini, F.; Pentimalli, M.; Delitala, C.; Scano, A.; Cabras, V.; Ferino, I. Liquid-Assisted Mechanochemical Synthesis of an Iron Carboxylate Metal Organic Framework and Its Evaluation in Diesel Fuel Desulfurization. *Microporous Mesoporous Mater.* 2015, 213, 14−21.

(23) Wang, L.; Zhang, F.; Wang, C.; Li, Y.; Yang, J.; Li, L.; Li, J. Ethylenediamine-Functionalized Metal Organic Frameworks MIL-100(Cr) for Efficient CO_2/N_2O Separation. *Sep. Purif. Technol.* 2020, 235, 116219.

(24) Yang, J.; Bai, H.; Zhang, F.; Liu, J.; Winarta, J.; Wang, Y.; Mu, B. Effects of Activation Temperature and Densification on Adsorption Performance of MOF MIL-100(Cr). *J. Chem. Eng. Data* 2019, 64, 5814−5823.

(25) Parker, S. F.; Fernandez-Alonso, F.; Ramirez-Cuesta, A. J.; Tomkinson, J.; Rudic, S.; Pinna, R. S.; Gorini, G.; Fernández Castañon, J. Recent and future developments on TOSCA at ISIS. *J. Phys.: Conf. Ser.* 2014, 554, 012003.

(26) Ryder, M. R.; Civalleri, B.; Bennett, T. D.; Henke, S.; Rudic, S.; Cinque, G.; Fernandez-Alonso, F.; Tan, J. C. Identifying the Role of Terahertz Vibrations in Metal-Organic Frameworks: From Gate-Opening Phenomenon to Shear-Driven Structural Destabilization. *Phys. Rev. Lett.* 2014, 113, 215502.

(27) Mahalakshmi, G.; Balachandran, V. FT-IR and FT-Raman Spectra, Normal Coordinate Analysis and Ab Initio Computations of Trimesic Acid. *Spectrochim. Acta, Part A* 2014, 124, 535−547.

(28) Griffin, A.; Jobic, H. Theory of the Effective Debye-Waller Factor in Neutron Scattering from High Frequency Molecular Modes. *J. Chem. Phys.* **1981**, *75*, 5940−5943.

(29) *Neutron Scattering - Fundamentals, Experimental Methods in the Physical Sciences*; Fernandez-Alonso, F., Price, D. L., Eds.; Academic Press: New York, 2013.

(30) Ryder, M. R.; Civalleri, B.; Cinque, G.; Tan, J.-C. Discovering Connections between Terahertz Vibrations and Elasticity Underpinning the Collective Dynamics of the HKUST-1 Metal-Organic Framework. *CrystEngComm* **2016**, *18*, 4303−4312.

(31) Souza, B. E.; Rudic, S.; Titov, K.; Babal, A. S.; Taylor, J. D.; Tan, J. C. Guest-Host Interactions of Nanoconfined Anti-Cancer Drug in Metal-Organic Framework Exposed by Terahertz Dynamics. *Chem. Commun.* **2019**, *55*, 3868−3871.

(32) Cunha, D.; Ben Yahia, M.; Hall, S.; Miller, S. R.; Chevreau, H.; Elkaïm, E.; Maurin, G.; Horcajada, P.; Serre, C. Rationale of Drug Encapsulation and Release from Biocompatible Porous Metal-Organic Frameworks. *Chem. Mater.* **2013**, *25*, 2767−2776.

(33) Chaudhari, A. K.; Kim, H. J.; Han, I.; Tan, J. C. Optochemically Responsive 2D Nanosheets of a 3D Metal-Organic Framework Material. *Adv. Mater.* **2017**, *29*, 1701463.

(34) Rastogi, V. K.; Palafox, M. A. Vibrational Spectra, Tautomerism and Thermodynamics of Anticarcinogenic Drug: 5-Fluorouracil. *Spectrochim. Acta, Part A* **2011**, *79*, 970−977.